11. Bruening-Wright, A., Elinder, F. & Larsson, H. P. *J. Gen. Physiol.* **130,** 71–81 (2007).
12. Kosta, S. P. *et al. Int. J. Med. Eng. Informatics* **3,** 16–29 (2011).
13. Reich, H. J. & Depp, W. A. *J. Appl. Phys.* **9,** 421 (1938).
14. Francis, V. *Fundamentals of Discharge Tube Circuits* (Methuen, 1948).
15. Richardson, O. W. *The Emission of Electricity from Hot Bodies* 1st edn, 304 (Longmans, Green and co., 1916).
16. Ayrton, H. M. *The Electric Arc* 479 ("The electrician" printing and publishing company, 1902).
17. Ayrton, H. M. *J. Institution of Electrical Engineers* **28,** 400–436 (1899).
18. Duddell, W. *J. Institution of Electrical Engineers* **30,** 232–267 (1901).
19. Duddell, W. *Phil. Trans. R. Soc. Lond. A* **203,** 305–342 (1904).
20. Frith, J. & Rodgers, C. On the resistance of the electric arc. *The London Philosophical Magazine* (1896).
21. Luggin, H. *Centralblatt für Elektrotechnik* (Munchen und Leipzig, 1888).
22. Pickett, M. D., Borghetti, J., Yang, J. J., Medeiros-Ribeiro, G. & Williams, R. S. *Adv. Mater.* **23,** 1730–1733 (2011).
23. Blondlot, M. R. *Comptes Rendus* **CIV,** 283 (1887).
24. Sapoff, M. & Oppenheim, R. M. in *Proc. IEEE* **51,** 1292–1305 (1963).
25. Faraday, M. *Experimental Researches in Electricity* (Bernard Quaritch, 1833).
26. Liao, Z-M. *et al. Small* **5,** 2377–2381 (2009).
27. Nayak, A. *et al. J. Phys. Chem. Lett.* **1,** 604–608 (2010).
28. Volta, A. *Phil. Trans. R. Soc. Lond.* **90,** 403–431 (1800).
29. Davy, H. *Nicholson's Journal of Natural Philosophy, Chemistry and the Arts* **4,** 326–328 (1800).
30. Davy, H. *The Journal of the Royal Institution of Great Britain* **I,** 166 (1802).
31. Davy, H. *Phil. Trans. R. Soc. Lond. C* 232–257 (1810).
32. Davy, H. *Elements of Chemical Philosophy* 511 (Bradford and Inskeep, 1812).
33. Chua, L. *Appl. Phys. A* **102,** 765–783 (2011).
34. Ohm, G. S. *Die Galvanische Kette, Mathematisch Bearbeitet* 250 (Kessinger, 1827).
35. Van Der Pol, B. & Van der Mark, J. *Nature* **120,** 363–364 (1927).

Acknowledgements

We acknowledge the financial support of Wilf Corrigan, the CHIST-ERA ERA-Net, EPSRC EP/J00801X/1, the Lindemann Trust, USA AFOSR grant FA9550-10-0290 and the Royal Academy of Engineering. We would also like to thank E. B. Haigh for her assistance in tracking historical evidence to support this work.

When Brownian diffusion is not Gaussian

Bo Wang, James Kuo, Sung Chul Bae and Steve Granick

It is commonly presumed that the random displacements that particles undergo as a result of the thermal jiggling of the environment follow a normal, or Gaussian, distribution. Here we reason, and support with experimental examples, that non-Gaussian diffusion in soft materials is more prevalent than expected.

Fickian diffusion is the dominant form of molecular and supramolecular transport. It is also the simplest time-dependent random process: a random walk for which the mean square displacement (MSD) is proportional to elapsed time. In fact, Einstein's celebrated analysis of Brownian motion assumes that big particles in a fast-moving small-molecule solvent follow random walks[1]. The assumption was based on an extreme separation of timescales — associated with the slow-moving particle and the fast-wiggling solvent molecules — which leads to the classic statistical-mechanics treatment embodying a coarse-grained fluctuating force as a Gaussian-distributed stochastic temporal series[2]. Indeed, when random walks are viewed as a succession of steps, it follows from the central limit theorem that for sufficiently long times the dynamics have to be Gaussian and the diffusion Fickian[3]. Yet recent direct observations in systems without a large separation of timescales — for example, the diffusion of colloids on phospholipid fluid tubules and in biofilament networks[4,5] (Fig. 1a) — repeatedly find the distribution of displacements in Fickian diffusion to deviate from Gaussian (Fig. 1b). System-specific interpretations have been proposed[6,7] but the finding of non-Gaussian Brownian diffusion calls for a general perspective.

Intriguingly, non-Gaussian probability distributions of mobility are increasingly recognized in a variety of physicochemical and socio-economical systems: Brownian motion in supercooled liquids[8–12] and close to jamming transitions[13–19], far-from-equilibrium systems such as granular gas and plasma[20–23], flow and drainage[24–28], friction[6,29,30], turbulence[31,32] and also financial and political fluctuations[33,34]. With this Commentary we wish to draw attention to the common thread: slowly varying, heterogeneous fluctuations of the environment (Fig. 1c) that lead to the observation of non-Gaussian behaviour at comparable or slower timescales than that for the onset of Fickian diffusion (Fig. 1d).

Patterns of non-Gaussian diffusion

As long as diffusion remains Fickian, non-Gaussian distributions of particle displacements (here denoted by the function $G_s(r,t)$, where $r(t)$ is the displacement at time t) spread proportionally to the square root of elapsed time and with the diffusion coefficient D. Generally, the central portion of a non-Gaussian distribution function can be approximated by a Gaussian function, $G_s(x,t) \propto \exp[-x^2/2\sigma^2(t)]$, with width σ and, where x is one-dimensional displacement whereas the remaining tail can roughly be described by an exponential curve, $G_s(x,t) \propto \exp[-|x|/\lambda(t)]$, with exponent $1/\lambda$, where λ is the characteristic decay length. Hence, the Gaussian centre and the exponential tail can be identified with hypothetical diffusion coefficients D_{Gauss} and D_{tail}, respectively, differing from the average diffusivity D. Decoupled diffusivities can be found for instance in random walks in dense colloidal suspensions, for which microscopic motion splits into trapped and hopping dynamics[10–13]. Yet the general phenomenology has been observed in a broader range of experimental and simulation work[4–34]. As illustrated in Fig. 2, $G_s(r,t)$ falls into four families according to whether the exponential tails are larger, comparable to, or smaller than the average diffusivity.

As to the temporal evolution of these distributions, there are notable general trends. Typically (but not exclusively) the central portion of the distribution

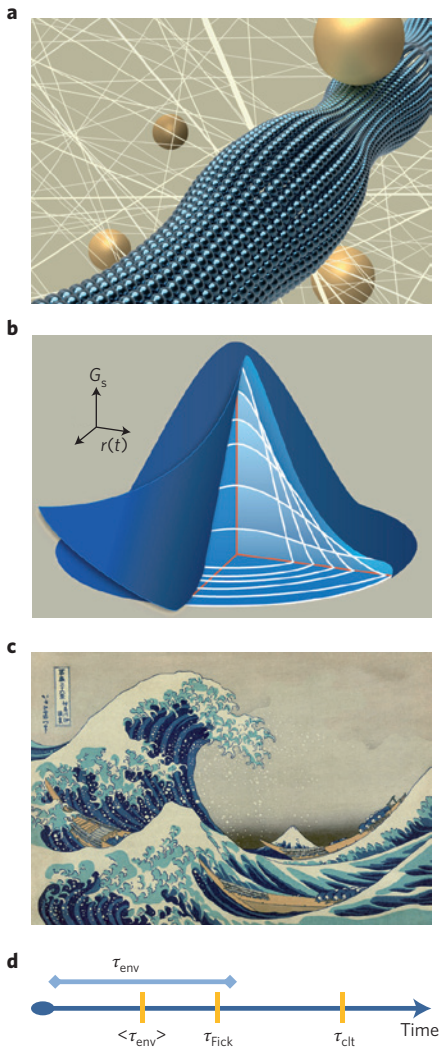

Figure 1 | Peculiarities of Brownian diffusion in soft materials where the environment fluctuates slowly on broad timescales. **a**, Slow environmental relaxation is common in soft matter, exemplified here by colloidal particles diffusing in an environment of biopolymer filaments and phospholipid tube assemblies. **b**, The distributions of displacements of objects diffusing a distance r in a certain time t in a slowly relaxing environment can be described with a non-Gaussian probability distribution function, $G_s(r,t)$, which can be decomposed into a set of elementary diffusive Gaussian processes (white curves). **c**, Environmental fluctuations can span a wide range of times (or frequencies), as illustrated by the woodcut print *The Great Wave* from the Japanese artist Katsushika Hokusai. **d**, We speculate that before the emergence of Gaussian behaviour at time τ_{clt} as ultimately demanded by the central limit theorem, Fickian diffusion should be observed starting at an earlier time, τ_{Fick}, which exceeds the average relaxation time of the environment, $<\tau_{env}>$, but not its full range of fluctuation. Panels: **a**, courtesy of Rui Lu; **c**, © Getty Images.

becomes less and less Gaussian with elapsed time when considering displacements normalized by the square root of time (this is consistent with the arguments presented below about convergence of underlying elementary fluctuations). During this time, motion is Brownian yet the system does not sample all possible dynamic states (in other words, for insufficiently long times, even Brownian motion is not ergodic). Of course, at sufficiently long times the distributions revert to Gaussian as dictated by the central limit theorem. For those cases in which the crossover from non-Gaussian to Gaussian distribution is observed with increasing time over experimentally accessible timescales, such as in nanoparticle diffusion on fluctuating lipid tubules[4], the reversion initiates at small normalized displacements. Non-Gaussian yet Fickian behaviour normally spans many decades in time, making the crossover to Gaussian difficult to access in experiments.

Liposome diffusion in nematic solutions

We next discuss non-Gaussian diffusion by way of a case study. Using single-particle tracking[4], we observed Fickian yet non-Gaussian diffusion of fluorescently tagged unilamellar lipid vesicles (liposomes) diffusing in (nematic) solutions of aligned F-actin filaments (see Methods for details on sample preparation and measurements).

We learned that in this system multiple non-Gaussian displacement distributions coexist. First, we observed Brownian trajectories uniaxially stretching in the direction of the nematic director (the direction parallel to the long axis of the filaments), as expected[35] (Fig. 3a). In fact, the angular dispersion of the nematic director agreed with that of a solution of F-actin filaments as reported before[36]. We then calculated the one-dimensional average MSD (Fig. 3b) and the displacement distributions (Fig. 3c), which show Fickian diffusion and non-Gaussian behaviour in both the parallel and perpendicular directions to the director. In the perpendicular direction the distribution shows exponential tails for times up to 2 s, whereas in the parallel direction the tails and the central portion of the distribution can be fitted with Gaussian functions, albeit of different widths. For longer time intervals, the central portion sharpened slightly whereas the tail spread as the square root of elapsed time ($\lambda^2 \propto t$ and $\sigma^2 \propto t$ for the perpendicular and parallel directions, respectively), implying $D^{\perp}_{tail} \approx 0.15\ \mu m^2\ s^{-1}$ and $D^{\parallel}_{tail} \approx 1.4\ \mu m^2\ s^{-1}$. In comparison, the average diffusivities corresponding to the MSD data are $D^{\perp}_{ave} = 0.45\ \mu m^2\ s^{-1}$ and $D^{\parallel}_{ave} = 1.1\ \mu m^2\ s^{-1}$. Although we expected Gaussian statistics at sufficiently long times, we did not observe this in the time window the experiments were carried out in, which was limited by the average time interval the liposomes stay within the depth of focus of the microscope. We attempted to access Gaussian diffusion through the alteration of the environmental dynamics, either by cutting the filaments down to 3 μm in length with gelsolin[37], which speeds up their longitudinal relaxation, or by adding Mg^{2+} ions up to a concentration of 16 mM, which causes transient bridging of neighbouring filaments[35]. However, both attempts caused negligible perturbations to liposome diffusion. Non-Gaussian behaviour seemed to robustly span broad timescales.

Physical meaning of non-Gaussianity

We propose that a simple and physically motivated interpretation of non-Gaussian diffusion can be attained if it is described by the convolution of Gaussian, independently diffusive processes[4]. In a general context, this is the statistical-mechanics approach of decomposing complex processes into normal modes, and it bears direct relevance to systems with different microscopic origins for the dynamic heterogeneity, such as activated hopping and turbulent flow (indeed, a parallel analysis of probability distribution functions in random flows was reported[32]). Mathematically,

$$G_s(x,t) = \int P(D) \cdot g(x \mid D) \cdot \mathrm{d}D \qquad (1)$$

where $P(D)$ is the effective distribution of diffusivities, which reflects physically the temporal correlation of microscopic fluctuations[2], and $g(x \mid D) = 1/\sqrt{4\pi Dt}\,\exp(-x^2/4Dt)$.

Equation (1) does not necessarily imply that non-Gaussian diffusive systems have multiple diffusion coefficients; after all, diffusivity is an averaged quantity. Instead, the independently diffusive processes pertain intermittently to the same diffusing object. This is supported by observations of positive time correlation for displacement amplitudes — large displacements are likely to be followed by large displacements — despite the absence of directional correlation[4].

Figure 4 shows the distribution of diffusivities $P(D)$ obtained from the displacement distribution $G_s(x,t)$ for the diffusion of liposomes in nematic solutions of actin filaments (see Methods). The sharp peak approaching zero diffusivity corresponds to the 'dynamically trapped' regime (slow diffusion), and the broad

peaks near the average diffusion coefficients indicate that that the environmental noise driving the motion of the probe (fast diffusion) can be decomposed into elements of a large spectral span. Here, the separation of the distribution of diffusivities into slow and fast portions does not necessarily indicate a decoupling into slow and fast particle populations, as commonly occurs in gels and glasses[14,18,38]; indeed, this is not observed in this system (Fig. 3a). Instead, we envisage that the separation and broad distribution of diffusivities stem from the heterogeneity of the environment, which is reflected in the dynamics of the probe[39]. The subtle difference between the spectra of diffusivities for the directions parallel and perpendicular to the filaments (Fig. 4a) becomes clear when they are plotted on semilogarithmic scales (Fig. 4b): the decay of the diffusivity curves past the broad peaks is slower for the perpendicular direction.

Interestingly, the spectra of diffusivities suggest a simple reason why exponential displacement distributions are often reported in the literature. For large D, $G_s(x,t)$ can be approximated by steepest descent analysis to $G_s(x,t) \sim \int 1/\sqrt{D} \cdot \exp[\ln(P(D)) - x^2/4Dt] \cdot dD$. In the limit of constant $\partial\ln(P(D))/\partial D$, $G_s(x,t)$ is exponential whereas it is closer to Gaussian when $\partial\ln(P(D))/\partial D$ is a strong function of D. In reality, the measured tails would fall between these two limits, yet because of the necessarily limited experimental dynamic range, the tails tend to appear exponential. In physical terms, the more heterogeneous the dynamics is in regimes of large amplitude, the closer to exponential the displacement distributions are anticipated to be.

Bound by the central limit theorem

Our analysis suggests criteria that can be used to guess the shortest timescale for which the displacement distribution becomes Gaussian, as ultimately required by the central limit theorem. If displacement fluctuations are composed of intrinsically non-Gaussian processes, then $P(D)$ is a mathematical transform of orthogonal fluctuation modes. Thus, the distribution function will converge to a Gaussian at times greater than the correlation time of the fluctuations. This should be the case for systems with 'coloured' noise — that is, noise with unevenly distributed frequencies — such as proteins diffusing on lipid membranes with power-law fluctuations[4,40]. In principle, this argument also applies to Brownian motion close to the transition from the ballistic to the diffusive regimes, when hydrodynamic memory

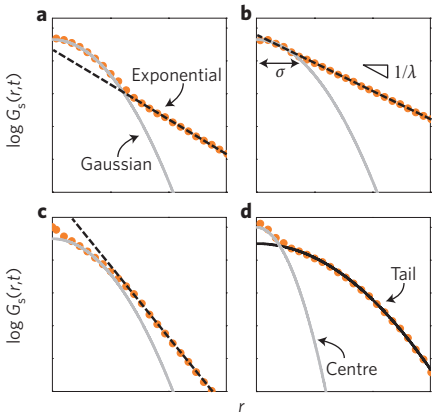

Figure 2 | Non-Gaussian yet Fickian diffusion can be described with four types of probability distributions, plotted here semilogarithmically against displacement. **a**–**c**, The central portion is commonly Gaussian with variance σ^2, but it is common to find tails described by exponential functions with exponents that scale with the square root of time, $\lambda(t) \propto \sqrt{t}$. The Gaussian centre and exponential tails can combine in three generic ways, depending on their relative position. **d**, It is also possible that the central and tail portions are both Gaussian but with different variance. For diffusion in two and three dimensions, the probability is usually normalized by sampling area ($2\pi r$ for two dimensions, $4\pi r^2$ for three dimensions). The dynamic range typically spans several decades in probability.

exerts 'coloured' thermal fluctuations with timescales comparable to those of diffusion[41]. Hence, it is reasonable to expect diffusive Brownian motion to be transiently non-Gaussian during the initial time of this transition. Still, this hypothesis needs to be tested.

However, if $P(D)$ characterizes displacement fluctuations arising from physical heterogeneity in time or space, or both, each elementary step in a random walk can be thought of as effectively sampling the convolution of all possible microscopic states, provided that the time and length scales of the step are larger than those of the heterogeneities. Therefore, when the environment relaxes more slowly than the time window in which measurements are performed (the characteristic time is of the order of seconds for the F-actin solution studied here[37,39]), the steps converge to an identical function only at longer timescales, and Gaussian behaviour emerges gradually at even longer times than are experimentally accessible. Of course, the argument supposes that $P(D)$ is invariant in time, but this is supported by the data in Fig. 4, and it seems physically unlikely that the distribution of diffusivities could evolve with time while maintaining a constant average value. This argument illustrates why non-Gaussian behaviour can reasonably be expected to span orders of magnitude in time.

A speculative look forward

Our analysis implies that the elementary processes underlying diffusive transport are stationary and ergodic at sufficiently long times — that is, at equilibrium. This hypothesis is supported by the experimental observations from two aspects. First, single-particle trajectories exhibited no variation beyond statistical spreading due to a finite number of data points, and second, no ageing in terms of dynamics was noticed. Therefore, our analysis does not apply to glasses and gels, notwithstanding the fact that the displacement distributions for these systems[11–18] (in some cases with exponential tails with $\lambda \propto \sqrt{t}$) and for the physical cases discussed here are alike. Actually, the similarity suggests that mobile particles in dynamically heterogeneous glassy systems might possess diffusive character. However, exploring this possibility will require experimental approaches that are capable of capturing with sufficient spatial and temporal resolution the large and rare displacements of mobile particles in glasses. In fact, in practice they have been considered as instantaneous hops[13].

It may be tempting to cast the current discussion in the context of the vast theoretical literature on sub-diffusion, in other words, of those diffusion processes for which MSDs grow sub-linearly with elapsed time. The major classes of stochastic models are the continuous-time random walk and the fractional Brownian motion[42,43]. Generally, continuous-time random walk assumes stochastic switching in time between two states — wait and jump — and leads to ergodicity breaking, and fractional Brownian motion assumes long-ranged temporal correlation of random fluctuations. Neither of these assumptions was confirmed in the systems that we have explored[4]. It is certainly true that it is possible to construct dynamics consistent with Fickian and non-Gaussian behaviour using these two models under special situations; for example, continuous-time random walk with truncated waiting-time distributions and finite jump-length variances. As this and similar lines of reasoning require additional assumptions about the temporal nature of the dynamical correlations, on physical grounds we expect that such detailed mechanisms should vary from system to

system. However, the phenomenological behaviour seems to be rather generic. Looking to the future, it is evident that this will be a worthwhile direction to pursue to statistically distinguish between detailed candidate mechanisms and to explore the physical grounds of various mathematical descriptions in a system-specific manner. As current mathematical reasoning has been aimed at describing sub-diffusion, not the Fickian diffusion emphasized here, it seems that progress in expanding currently available statistical measures[44,45] can be expected.

Clearly, assuming that Fickian processes are Gaussian may lead to erroneous conclusions, in particular for small systems for which sampled displacement data may fall in the central, Gaussian portion of the non-Gaussian displacement probability distribution. This is an underappreciated pitfall that is often made in the interpretation of data from single-molecule imaging. The assumption of an underlying Gaussian process can also lead to errors when performing the inversion of displacement measurements, which is common practice when analysing scattering data obtained in Fourier space, for example.

With these issues in mind, we emphasize the experimental desirability of accumulating huge data sets, spanning orders of magnitude of probability distribution so as to reveal rare events. Admittedly, this can be tedious, yet it is often crucial to discriminate the nature of particle motion, particularly when the dynamics is heterogeneous, or not in equilibrium. Large statistics of this sort have become manageable to gather from single-particle tracking[4,39], as illustrated in Fig. 3; the spirit is to image thousands or even millions of trajectories without pre-selection. Moreover, transparent weighting analysis enables reconstruction of the dynamic path in trajectory space[38,46], where dynamics are not only associated with time and space, but also history.

From a practical viewpoint, it is fair to ask why all this matters, as the non-Gaussian character mostly appears in the tails of the distributions, and thus with low probability. The answer is that this can be at the heart of the understanding of the physics of soft-matter systems, especially in those where rare events dominate the long-time dynamics. Apart from classical examples, such as relaxation, transport and reaction in complex media[47–50], we anticipate intriguing developments in materials science involving triggered actions in which diffusion, in a first step of a process, sets off a cascade of subsequent processes. In biology there are many examples of this, such as signalling and metabolite shuttling[51], and materials scientists are discovering the usefulness of triggered actions in applications involving pathway-dependent or kinetically controlled processes[52,53]. Furthermore, the emerging field of active matter concerns itself with internally driven systems that sample rare events more frequently[5,7,54–56], likewise highlighting the significance of non-Gaussian distributions. Even more broadly, we envisage that in systems with first-passage processes — such as targeting, translocation, triggering, criticality and resonance[57,58] — rare fluctuations may dominate the systems' dynamics and induce relevant transitions. Certainly, Fickian yet non-Gaussian diffusion will lead us to the discovery of unexpected phenomena.

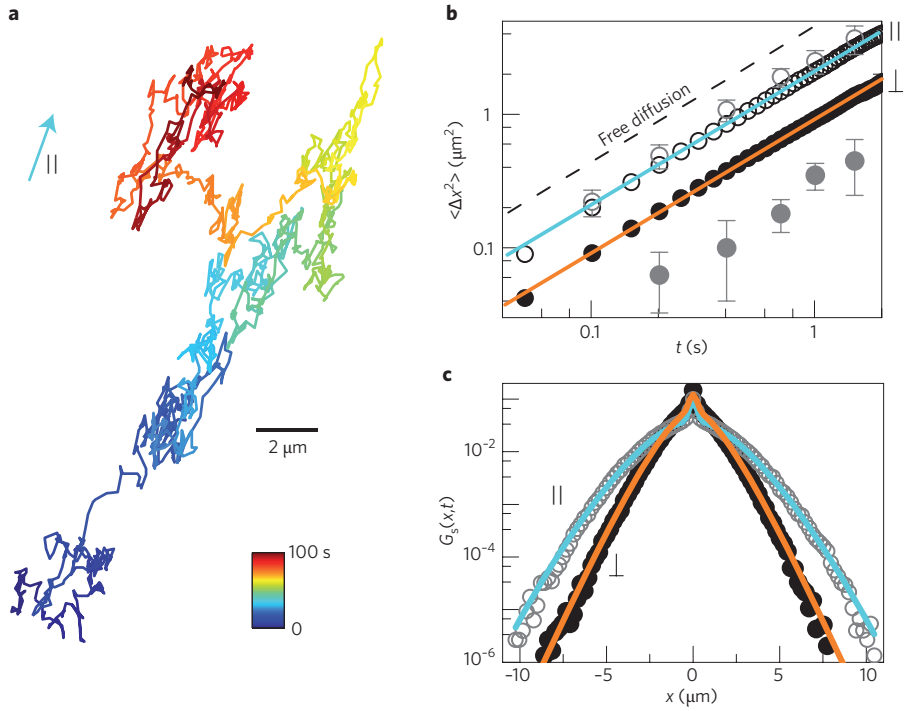

Figure 3 | Liposome diffusion in a nematic solution of F-actin filaments. **a**, Two-dimensional projection of a typical 100 s trajectory (50 ms between frames) of PEG-stabilized liposomes measured with an epifluorescence microscope focused deep into the sample. Colours denote the time lapse of the trajectory. The orientation of the trajectory (the director, denoted by the arrow) was determined from the first principal component of the frame-to-frame displacement vectors. **b**, A logarithmic plot of the MSD of the liposomes in the directions parallel (open circles and cyan line) and perpendicular (filled circles and orange line) to the filaments shows linear time dependence with slopes of 1, and thus Fickian diffusion ($\langle\Delta x^2(t)\rangle = 2Dt$ with $D^{\parallel}_{ave} = 1.1\ \mu m^2\ s^{-1}$ and $D^{\perp}_{ave} = 0.45\ \mu m^2\ s^{-1}$). Included is the free-diffusion limit — that is, the MSD of liposomes in water without actin (dashed line; $D_0 = 2.2\ \mu m^2\ s^{-1}$) — and the hypothetical MSDs (grey symbols) inferred from the tails of the displacement probability distributions shown in **c**. The error bars show the standard deviations estimated by bootstrapping of the trajectories. Data are shown up to a time interval of 3 s because for longer times a significant fraction of liposomes have diffused out of the focus of the microscope. **c**, Measured displacement probability distributions for a 2 s time interval show that diffusion parallel to the filaments is Gaussian (albeit with different variance for the central and tail portions), whereas the exponential tails of the distribution in the perpendicular direction imply slower diffusion ($D^{\parallel}_{tail} \approx 1.4\ \mu m^2\ s^{-1}$ and $D^{\perp}_{tail} \approx 0.15\ \mu m^2\ s^{-1}$). Lines are best fits to the data points with equation (1).

Methods

Sample preparation and particle tracking. Following N_2 drying and hydration of the lipids, liposomes dyed with 2% N-(lissamine-rhodamine B)-dioleoylphosphatidylethanolamine (RhB-DOPE) were prepared through a two-step ultrasonication procedure: bath sonication for 10 min, and tip sonication for 1 min (Branson sonifier at 65% amplitude, that is, at a power of 13–14 W). Then the suspensions were forced through polycarbonate filter membranes with a pore size of ~100 nm. Using dynamic light scattering we determined that the liposomes were 90±10 nm in size. The osmotic pressure across the membranes was balanced by

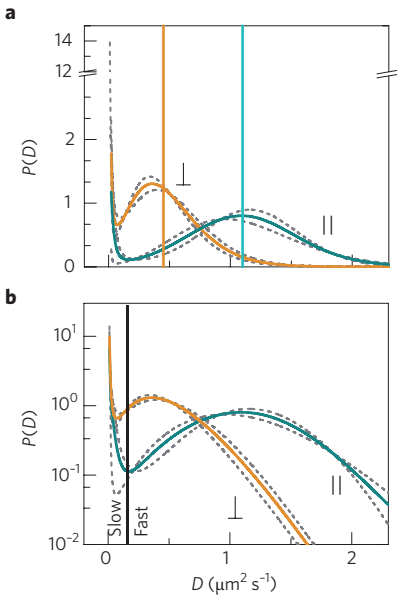

Figure 4 | Non-Gaussian yet Fickian diffusion is reflected in the spectrum of diffusivities underlying liposome diffusion in a nematic solution of actin filaments. **a**,**b**, The probability distributions of diffusivities, $P(D)$, inferred by inverting the non-Gaussian probability distributions of liposome displacements (see Methods), are plotted linearly (**a**) and semilogarithmically (**b**) for motion perpendicular (orange) and parallel (cyan) to the actin filaments. The small differences between inferences from 200 ms and 2 s intervals (dashed lines) stem from numerical errors of the inversion procedure. Vertical lines in panel **a** indicate the average diffusivities, $D^{\parallel}_{ave} = 1.1\ \mu m^2\ s^{-1}$ and $D^{\perp}_{ave} = 0.45\ \mu m^2\ s^{-1}$, obtained from the measured MSDs. The dividing vertical line in panel **b** separates the 'slow' sharp peak and the 'fast' broad peak, which suggest independently diffusive processes acting intermittently on the liposomes.

preparing the liposomes in the same buffer used for actin polymerization. To avoid unwanted complications from specific interactions between the liposomes and actin, we stabilized the zwitterionic DOPC (1,2-dioleoyl-*sn*-glycero-3-phosphocholine) membranes with the lipid–polyethylene glycol conjugate DOPE-PEG (1,2-dioleoyl-*sn*-glycero-3-phosphoethanolamine-N-[methoxy(polyethylene glycol)-750]) at the high molar concentration of 10%. To characterize unspecific adsorption, the unlabelled liposomes were incubated with fluorescently labelled bovine serum albumin overnight to determine whether the protein segregates to the liposome surface. Freshly prepared liposomes were mixed into reconstituted G-actin suspensions (5 mg ml^{-1}) in fresh G-buffer (5 mM TRIS (tris(hydroxymethyl) aminomethane) at pH 8.0, supplemented with 0.2 mM $CaCl_2$, 1 mM ATP, and 0.2 mM dithiothreitol and 0.01% NaN_3). The polymerization of F-actin was initiated by adding salt (100 mM KCl, 2 mM $MgCl_2$) followed by equilibration on the microscope stage overnight at room temperature. Under these conditions, the filaments have an average contour length of ~21 μm (ref. 36). Using an epifluorescence microscope, we measured the vesicles' time-dependent positions with 20-nm precision[4], focusing deep into the sample (>100 μm; air objective, ×40 magnification, numerical aperture = 0.60) to avoid potential effects from the container's walls. Trajectories were generated by a program written in house[4].

Computation of the distribution of diffusivities. Using Lucy's iterative algorithm[59] — a technique widely used for deconvolution in signal processing — the distribution of diffusivities $P(D)$ in equation (1) can be computed from inverting the displacement distribution $G_s(x,t)$. For the $(n+1)$th iteration,

$$P^{n+1}(D) = P^n(D)\int \frac{G_s(x,t)}{G_s^n(x,t)}\, g(x \mid D)\mathrm{d}x \qquad (2)$$

where $G_s^n(x,t) = \int_0^{D_0} P^n(D)\cdot g(x \mid D)\mathrm{d}D$ is the nth approximation of the displacement distribution and D_0 is the coefficient corresponding to the free-diffusion limit. Equation (2) is bound by the constraints $\int_0^{D_0} P(D)\mathrm{d}D = 1$ and $P(D) \geq 0$. The initial condition $P^1(D) = 1/D_{ave}\cdot\exp(-D/D_{ave})$, for which equation (1) can be solved analytically, helps the algorithm to converge faster to a solution. ❐

Bo Wang[1], James Kuo[2], Sung Chul Bae[1] and Steve Granick[1]* are at the [1]Department of Materials Science and Engineering, University of Illinois, Urbana, Illinois 61801, USA; [2]Department of Chemical and Biomolecular Engineering, University of Illinois, Urbana, Illinois 61801, USA.*
**e-mail: sgranick@illinois.edu; bowang4@illinois.edu*

References

1. Frey, E & Kroy, K. *Ann. Phys.* **14,** 20–50 (2005).
2. Kubo, R. *Rep. Prog. Phys.* **29,** 255–284 (1966).
3. Tsallis, C., Levy, S. V. F., Souza, A. M. C. & Maynard, R. *Phys. Rev. Lett.* **75,** 3589–3593 (1995).
4. Wang, B., Anthony, S. M., Bae, S. C. & Granick, S. *Proc. Natl Acad. Sci. USA* **106,** 15160–15164 (2009).
5. Leptos, K. C., Guasto, J. S., Gollub, J. P., Pesci, A. I. & Goldstein, R. E. *Phys. Rev. Lett.* **103,** 198103 (2009).
6. Menzel, A. M. & Goldenfeld, N. *Phys. Rev. E* **84,** 011122 (2011).
7. Kurtuldu, H., Guasto, J. S., Johnson, K. A. & Gollub, J. P. *Proc. Natl Acad. Sci. USA* **108,** 10391–10395 (2011).
8. Eaves, J. D. & Reichman, D. R. *Proc. Natl Acad. Sci. USA* **106,** 15171–15175 (2011).
9. Stariolo, D. A. & Fabricius, G. *J. Chem. Phys.* **125,** 064505 (2006).
10. Saltzman, E. J. & Schweizer, K. S. *Phys. Rev. E* **77,** 051504 (2008).
11. Weeks, E. R., Crocker, J. C., Levitt, A. C., Schofield, A. & Weitz, D. A. *Science* **287,** 627–631 (2000).
12. Kegel, W. K. & van Blaaderen, A. *Science* **287,** 290–293 (2000).
13. Chaudhuri, P., Berthier, L. & Kob, W. *Phys. Rev. Lett.* **99,** 060604 (2007).
14. Gao, Y. & Kilfoil, M. L. *Phys. Rev. Lett.* **99,** 078301 (2007).
15. Hurtado, P. I., Berthier, L. & Kob, W. *Phys. Rev. Lett.* **98,** 135503 (2007).
16. Bray, D. J., Swift, M. R. & King, P. J. *Phys. Rev. E* **75,** 062301 (2007).
17. Castillo, H. E. & Parsaeian, A. *Nature Phys.* **3,** 26–28 (2007).
18. Yu, Y., Anthony, S. M., Bae, S. C. & Granick, S. *J. Phys. Chem. B* **115,** 2748–2753 (2011).
19. Marty, G. & Dauchot, O. *Phys. Rev. Lett.* **94,** 015701 (2005).
20. Chen, W. & To, K. *Phys. Rev. E* **80,** 061305 (2009).
21. Van Zon, J. S. & MacKintosh, F. C. *Phys. Rev. Lett.* **93,** 038001 (2004).
22. Rouyer, F. & Menon, N. *Phys. Rev. Lett.* **85,** 3676–3679 (2000).
23. Liu, B. & Goree, J. *Phys. Rev. Lett.* **100,** 055003 (2008).
24. Orpe, A. V. & Kudrolli, A. *Phys. Rev. Lett.* **98,** 238001 (2007).
25. Moka, S. & Nott, P. R. *Phys. Rev. Lett.* **95,** 068003 (2005).
26. Choi, J., Kudrolli, A., Rosales, R. R. & Bazant, M. Z. *Phys. Rev. Lett.* **92,** 174301 (2004).
27. Arévalo, R., Garcimartín, A. & Maza, D. *Eur. Phys. J. E* **23,** 191–198 (2007).
28. Reis, P. M., Ingale, R. A. & Shattuck, M. D. *Phys. Rev. E* **75,** 051311 (2007).
29. Touchette, H., van der Straeten, E. & Just, W. *J. Phys. A* **43,** 445002 (2010).
30. Goohpattader, P. S. & Chaudhury, M. K. *J. Chem. Phys.* **133,** 024702 (2010).
31. Shraiman, B. I. & Siggia, E. D. *Nature* **405,** 639–646 (2000).
32. Shraiman, B. I. & Siggia, E. D. *Phys. Rev. E* **49,** 2912–2917 (1994).
33. Silva, A. C., Prange, R. E. & Yakovenko, V. M. *Physica A* **344,** 227–235 (2004).
34. Majumder, S. R., Diermeier, D., Rietz, T. A. & Amaral, L. A. N. *Proc. Natl Acad. Sci. USA* **106,** 679–684 (2009).
35. He, J., Mak, M., Liu, Y. & Tang, J. X. *Phys. Rev. E* **78,** 011908 (2008).
36. Viamontes, J., Narayanan, S., Sandy, A. R. & Tang, J. X. *Phys. Rev. E* **73,** 061901 (2006).
37. Liu, J. *et al. Phys. Rev. Lett.* **96,** 118104 (2006).
38. Hedges, L. O., Jack, R. L., Garrahan, J. P. & Chandler, D. *Science* **323,** 1309–1313 (2009).
39. Wang, B. *et al. Phys. Rev. Lett.* **104,** 118301 (2010).
40. Reister-Gottfried, W., Leitenberger, S. M. & Seifert, U. *Phys. Rev. E* **81,** 031903 (2010).
41. Franosch, T. *et al. Nature* **478,** 85–88 (2011).
42. Metzler, R. & Klafter, J. *Phys. Rep.* **339,** 1–77 (2000).
43. Burov, S., Jeon, J-H., Metzler, R. & Barkai, E. *Phys. Chem. Chem. Phys.* **13,** 1800–1812 (2011).
44. Magdziarz, M., Weron, A., Burnecki, K. & Klafter, J. *Phys. Rev. Lett.* **103,** 180602 (2009).
45. Tejedor, V. *et al. Biophys. J.* **98,** 1364–1372 (2010).
46. Wu, D. *et al. Phys. Rev. Lett.* **103,** 050603 (2009).
47. Schweizer, K. S. *Curr. Opin. Colloid Interface Sci.* **12,** 297–306 (2007).
48. Ribière, P. *et al. Phys. Rev. Lett.* **95,** 268001 (2005).
49. Elf, J., Li, G-W. & Xie, X. S. *Science* **316,** 1191–1194 (2007).
50. Bénichou, O., Chevalier, C., Klafter, J., Meyer, B. & Voituriez, R. *Nature Chem.* **2,** 472–477 (2010).
51. Eldar, A. & Elowitz, M. B. *Nature* **467,** 167–173 (2010).
52. Chen, Q. *et al. Science* **331,** 199–202 (2011).
53. Korevaar, P. A. *et al. Nature* **481,** 492–496 (2012).
54. Romanczuk, P. & Schimansky-Geier, L. *Phys. Rev. Lett.* **106,** 230601 (2011).
55. Lin, L. C-L., Gov, N. & Brown, F. L. *J. Chem. Phys.* **124,** 074903 (2006).
56. Brangwynne, C. P., MacKintosh, F. C. & Weitz, D. A. *Proc. Natl Acad. Sci. USA* **104,** 16128–16133 (2007).
57. Condamin, S., Bénichou, O., Tejedor, V., Voituriez, R. & Klafter, J. *Nature* **450,** 77–80 (2007).
58. González, M. C., Hidalgo, C. A. & Barabási, A-L. *Nature* **453,** 779–782 (2007).
59. Lucy, L. B. *Astron. J.* **79,** 745–754 (1974).

Acknowledgements

We are indebted to Mykyta V. Chubynsky, Gary W. Slater, Sergey Panyukov, Michael Rubinstein and Raymond E. Goldstein for useful discussions. This work was supported by the US Department of Energy, Division of Materials Science, under Award DEFG02-02ER46019.